Supplemental Material

Dominant negative effects of *SCN5A* missense variants

Matthew J. O'Neill[1], Ayesha Muhammad[1], Bian Li[2], Yuko Wada[2], Lynn Hall[2], Joseph F. Solus[2], Laura Short[2],

Dan M. Roden[3†], Andrew M. Glazer[2*†]

Supplemental Methods.

Supplemental References.

Supplemental Data. Variant-level data from automated patch clamp.

1

Supplemental Methods

Western Blot: Cells either stably expressing an Na$_V$1.5 or an empty plasmid were homogenized in modified RIPA buffer (25 mM Tris-HCl, 150 mM NaCl, 5% glycerol, 1 mM EDTA, and 1% NP-40) supplemented with a protease inhibitor cocktail (cOmplete Mini, Roche) on ice. After centrifuge at 13000 rpm for 20 minutes at 4oC followed by colorimetric protein quantitation (Pierce 660 nm Protein Assay, #22660, #22662), the sample equivalent to 5 µg protein was denatured in LDS sample buffer (NuPAGE) with 1 mM DTT for 20 minutes at 70oC and separated in a 10% gel (Mini-PROTEAN TGX gel, BIO-RAD) by SDS-PAGE. After transferred to a PVDF membrane (0.45 µm, GE Healthcare) in Tris-Glycine buffer with 20% methanol followed by blocking with 5% skim milk for an hour at RT, the blot was incubated overnight at 4oC with anti-NaV1.5 antibody (1:1,000, Cell Signaling Technology, #14421), anti-mCherry antibody (1:1,000, Cell Signaling Technology, #43590), or anti-β-actin antibody (1:4,000, Cell Signaling Technology, #3700) in 0.1% TBST. After secondary antibody treatment (Promega, #W4011, #W4021), protein signal was detected by chemiluminescence (Clarity ECL Western Blotting Substrates, BIO-RAD).

Structural Analysis: Na$_V$1.5 variant locations were determined from UniProt[1]. The structural model of human SCN5A (UniProtKB: Q14524-1, modeled residues: 30–440, 685–957, 1174–1887) was generated by homology modeling using the protein structure prediction software Rosetta (v.3.10)[2]. The cryo-EM structure of human SCN9A bound with SCN1B and the Ig domain of SCN2B resolved to 3.2 Å (PDB: 6J8H)[3] were used as the primary templates while the cryo-EM structure of NavPaS from American Cockroach resolved to 2.6 Å (PDB: 6A95)[4] was used as a secondary template. The percent identity between the aligned positions of SCN9A and SCN5A sequences is 76.7%. While the percent identity between NavPaS and SCN5A was only moderate (45.6%), the N-terminal and C-terminal domains in the NavPaS structure were partially resolved, providing coordinates for modeling the corresponding domains of SCN5A. For further details, see our previous report[5]. Recently, an experimental structure of SCN5A was determined using cryo-EM technique at a resolution of 3.3 Å[6]. We note that the root-mean-square distance between our model and the experimental structure over all backbone atoms is 2.3 Å (Figure S1), suggesting that our model is accurate while covering more residues than the experimental structure.

Supplemental Case-Control Analyses: We performed an additional analysis restricting the controls to individuals of Non-Finnish European ancestry (NFE) in gnomAD and restricting the cases from the BrS consortium to Europeans. We performed the analysis with the same variant frequency thresholds, same calculation of odds ratios, and same allele number calculations after filtering for NFE. To perform a sensitivity analysis, we recalculated odds ratios at various threshold of the dominant negative effect spanning 0.50 to 0.80 by increments of 0.05.

**Table S1. Variant currents and case-control counts.**

Variant	Homozygous Peak Current Density	S.E.	Cells	Heterozygous Peak Current Density	S.E.	Cells	gnomAD Count	gnomAD MAF	Walsh Count
WT	100	1.3	1950	100	1.3	246	-	-	-
WT+WT	-	-	-	218.4	7.7	199	-	-	-
p.Gly1262Ser	46.5	15.5	10	231.6	10.8	47	8	2.83E-05	3
p.Glu746Lys	46.1	11.8	9	213.3	9.5	45	6	2.14E-05	5
p.Ser1218Ile	13.9	2.4	19	176.6	9.8	47	1	4.02E-06	0
p.Glu1225Lys	40.6	7	19	170.8	12	43	1	4.01E-06	5
p.Leu136Pro	34.7	6.3	16	167.8	9.7	41	0	0	2
p.Gly1406Arg	33.6	3.7	18	145.6	12.5	35	0	0	3
p.Pro1730His	45.1	5.1	31	139.5	9	47	0	0	0
p.Trp822Ter	4.7	0.9	16	134.2	5.2	164	0	0	0
p.Val1405Leu	18.6	3.7	15	121.2	7.8	53	0	0	4
p.Glu1574Lys	38.7	12.8	8	119.9	7.6	46	0	0	3
p.Gly1661Arg	5.6	1.5	19	112	9.4	44	0	0	3
p.Ser1672Tyr	1	0.6	18	100.8	8.7	47	0	0	1
p.Arg893Cys	8.2	0.9	48	76.8	10.8	52	3	1.06E-05	2
p.Asn1722Asp	39.2	4.3	26	74.4	5.4	43	0	0	1
p.Thr187Ile	0.2	0.1	42	73.5	10.7	39	0	0	1
p.Ser910Leu	1.2	0.2	19	71.8	13.9	35	1	3.99E-06	3
p.Met369Lys	3.7	0.9	22	69.8	10.1	51	0	0	2
p.Arg104Trp	0.5	0.2	24	69.6	7.3	43	1	4.01E-06	3
p.Arg104Gln	0.4	0.2	22	68.3	6.1	34	0	0	3
p.Leu928Pro	1.4	0.9	27	66.3	6.8	47	0	0	1
p.Leu839Pro	3.1	2.2	20	63.5	10.5	53	0	0	1
p.Leu846Arg	0.3	0.2	43	63.5	7.9	35	0	0	0
p.Arg282His	20.2	3	16	63.4	6.6	44	4	1.60E-05	8
p.Leu325Arg	20.7	2.3	36	63.3	7.3	49	0	0	0
p.Phe892Ile	0.9	0.7	23	60.4	6.5	51	0	0	1
p.Gly1420Val	0	0	11	59.5	8	52	0	0	1
p.Arg367Cys	0.6	0.3	25	59.3	11.2	54	3	1.07E-05	3
p.Phe93Ser	0.2	0.2	15	58.8	7.7	53	0	0	1
p.Gly897Glu	0.8	0.3	16	58.1	9.9	38	0	0	0
p.Leu1346Pro	2.1	0.9	15	57.9	8.4	53	0	0	1
p.Gly1740Arg	29.8	2.8	20	53.6	8	27	0	0	1
p.Arg121Trp	0.7	0.3	40	52.7	8.4	36	0	0	3
p.Leu276Gln	1.1	0.8	14	50.8	10.1	53	0	0	2
p.Ser1382Ile	4.5	1	29	49.1	8.9	47	0	0	1
p.Arg282Cys	1.4	0.3	67	48.6	10	55	0	0	2
p.Glu901Lys	3.3	0.6	16	48.3	10.5	46	0	0	6
p.Ala735Glu	1.3	0.9	12	46.4	7.9	39	0	0	0
p.Arg878His	0.2	0.1	38	44.9	9.1	39	0	0	3
p.Ala1428Val	0.3	0.3	24	38.9	7	53	0	0	1
p.Gly1420Arg	2.5	1.2	16	36.1	9.9	50	0	0	2
p.Val1405Met	30	5.9	14	35.7	4.2	38	0	0	5
p.Asp1430Asn	0.4	0.1	57	34.5	9.6	28	0	0	0
p.Trp879Arg	0	0	43	30.9	6.5	46	0	0	0
p.Arg367Leu	0	0	39	30.3	9.6	46	0	0	1
p.Gly386Arg	1.5	0.9	11	29.2	7.2	52	0	0	0
p.Asn1380Lys	0.1	0.1	25	27.8	6.4	42	0	0	1
p.Gly1743Glu	1	0.4	11	27.5	7.1	37	0	0	5
p.Cys335Arg	0	0	24	26.5	8.4	27	0	0	1
p.Asp785Asn	36.9	6.7	27	24.7	5.6	33	0	0	0
p.Asp356Asn	1.4	0.3	16	19.3	3.6	45	1	4.02E-06	5
p.Gly1712Cys	8.3	2.4	17	13.9	3.3	38	0	0	0

Table S2 – Primers used in this Study.

Variant	Name	Sequence
p.Phe93Ser	ag738	CTATAGCACCCAAAAGACTTCCATCGTACTGAATAAAGGCA
p.Arg104Gln	ag1122	GGCAAGACCATCTTCCAGTTCAGTGCCACCAAC
p.Arg104Trp	ag885	GGCAAGACCATCTTCTGGTTCAGTGCCACCA
p.Arg121Trp	ag655	CTTCCACCCCATCTGGAGAGCGGCTGT
p.Leu136Pro	ag740	CTCGCTCTTCAACATGCCCATCATGTGCACCATCC
p.Thr187Ile	ag1123	CCTGCACGCATTCATTTTCCTTCGGGACC
p.Leu276Gln	ag742	CTCTTCATGGGCAACCAAAGGCACAAGTGCGTG
p.Arg282Cys	ag729	GGCACAAGTGCGTGTGCAACTTCACAGCG
p.Arg282His	ag1124	GCACAAGTGCGTGCACAACTTCACAGCGC
p.Leu325Arg	ag884	CACCTCTGATGTGTTACGGTGTGGGAACAGCTCTG
p.Cys335Arg	ag785	GACGCTGGGACACGTCCGGAGGGCT
p.Asp356Asn	ag1125	GGCTACACCAGCTTCAATTCCTTTGCCTGGG
p.Arg367Cys	ag778	TTTCTTGCACTCTTCCTCCTGATGACGCAGGAC
p.Arg367Leu	ag665	CTTTCTTGCACTCTTCTGCCTGATGACGCAGGA
p.Met369Lys	ag743	CTCTTCCGCCTGAAGACGCAGGACTGC
p.Gly386Arg	ag745	AGACCCTCAGGTCCGCAAGGAAGATCTACATG
p.Ala735Glu	ag746	CAACACACTCTTCATGGAGCTGGAGCACTACAACA
p.Glu746Lys	ag669	GCGGCCGCGAATTCAAGGAGATGCTGCA
p.Asp785Asn	ag748	AGGGCTGGAACATCTTCAACAGCATCATCGTCATC
p.Trp822Ter	ag68	GCTGGCCAAATCATGACCCACCCTGAACACA
p.Leu839Pro	ag749	CAGTGGGGGCACCGGGGAACCTGAC
p.Leu846Arg	ag1126	AACCTGACACTGGTGCGTGCCATCATCGTGTTC
p.Arg878His	ag1127	GGCCTGCTGCCTCACTGGCACATGATG
p.Trp879Arg	ag798	CCTGCTGCCTCGCAGGCACATGATGGA
p.Phe892Ile	ag750	GCCTTCCTCATCATCATCCGCATCCTCTGTG
p.Arg893Cys	ag1128	CTTCCTCATCATCTTCCACATCCTCTGTGGAGAGT
p.Gly897Glu	ag1129	TCCGCATCCTCTGTGAAGAGTGGATCGAGAC
p.Glu901Lys	ag678	CTGTGGAGAGTGGATCAAGACCATGTGGGACTG
p.Ser910Leu	ag1130	GGACTGCATGGAGGTGTTGGGGCAGTC
p.Leu928Pro	ag782	TATGGTCATTGGCAACCCTGTGGTCCTGAATCTCT
p.Ser1218Ile	ag1131	TCATGATCCTACTCATCAGTGGAGCGCTGGC
p.Glu1225Lys	ag687	GGAGCGCTGGCCTTCAAGGACATCTACCTAG
p.Gly1262Ser	ag690	TCAAGTGGGTGGCCTACAGCTTCAAGAAGTACTTC
p.Leu1346Pro	ag754	CTGCCTCATCTTCTGGCCCATCTTCAGCATCATGG
p.Asn1380Lys	ag755	TTTGAACTACACCATCGTGAACAAAAAGAGCCAGTGTG
p.Ser1382Ile	ag795	CTACACCATCGTGAACAACAAGATCCAGTGTGAGTC
p.Val1405Leu	ag756	AGTCAACTTTGACAACCTGGGGGCCGGGTA
p.Val1405Met	ag757	AAAGTCAACTTTGACAACATGGGGGCCGGGTAC
p.Gly1406Arg	ag1132	CTTTGACAACGTGCGGGCCGGGTACCT
p.Gly1408Arg	ag1133	ACGTGGGGGGCCAGGTACCTGGCC
p.Gly1420Val	ag760	GCAGGTGGCAACATTTAAAGTCTGGATGGACATTATGTATG
p.Gly1420Arg	ag759	GTCCATCCAGCGTTTAAATGTTGCCACCTGCAG
p.Ala1428Val	ag761	GGACATTATGTATGCAGTTGTGGACTCCAGGGGG
p.Asp1430Asn	ag1134	TTATGTATGCAGCTGTGAACTCCAGGGGGTATGAA
p.Gly1661Arg	ag645	GCCCTCTTCAACATCAGGCTGCTGCTCTTCC
p.Ser1672Tyr	ag766	CGTCATGTTCATCTACTACATCTTTGGCATGGCCA
p.Asn1722Asp	ag791	AGCCCCATCCTCGACACTGGGCCGC
p.Pro1730His	ag793	CCCTACTGCGACCACACTCTGCCCAAC
p.Gly1743Glu	ag036	TCTCGGGGGGACTGCAGGAGCCCAGCCGTGG

5

Table S3. Case-control analysis.

Class	# of variants	BrS cohort count	gnomAD count	gnomAD AF	BrS : gnomAD ratio	Odds Ratio
All missense	300	411	1483	5.9e-3	0.28	11.0
In-frame indel	19	15	22	8.7e-5	0.68	24.2
Frameshift+splice	127	153	48	4.2e-4	3.19	118
Missense LoF + Dom. Neg.	32	54	6	2.3e-5	9.0	323
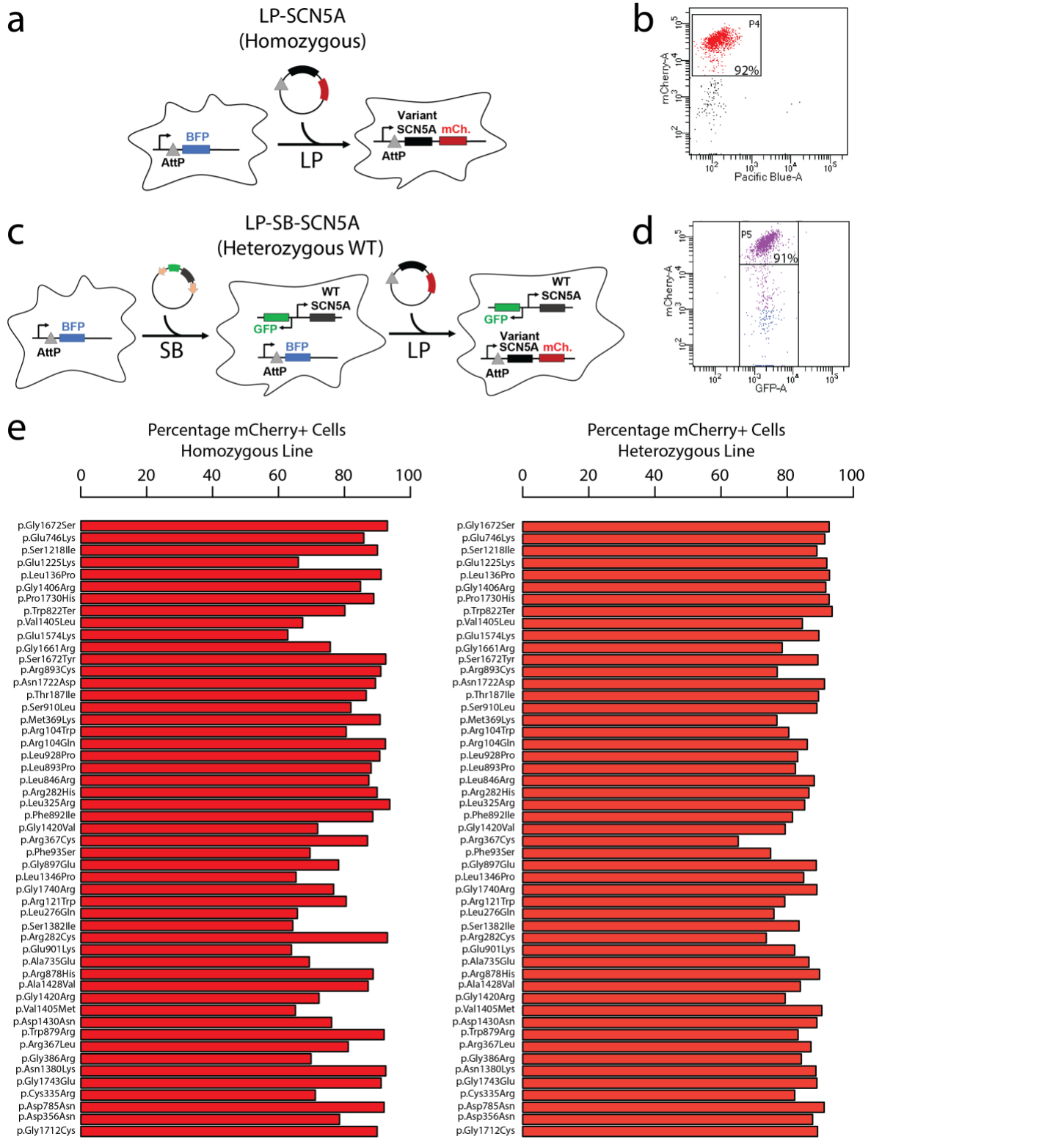
Figure S1. Stable cell lines used in this study and flow cytometry expression reporters. 1 or 2 copies of *SCN5A* were inserted into engineered HEK293 LP cells. The Landing Pad (LP) comprises an AttP and BFP locus, and allows insertion of a single insert per cell. A second Sleeping Beauty (SB) transposon system was used to introduce a second copy of the gene for heterozygous experiments.

a Design of homozygous LP-SCN5A cell line with LP integration.

b Analytical flow cytometry after incorporation of plasmid into the LP. Cells that do not have BFP expression and highly express mCherry (P4 gate) have a successful integration and serve as a marker of channel expression.

c For heterozygous experiments, we used a combination of LP and SB systems. First, a SB plasmid bearing a WT copy of *SCN5A* was randomly inserted into the genome. A clone of these cells was identified that has an equal level of Na$_V$1.5 in patch clamp experiments to typical LP expression (Figure 2). Next, a second copy of *SCN5A* bearing WT or variant was incorporated through the LP system.

d Results of flow cytometry after SP and LP integration. Cells express GFP associated with SB integration, and mCherry after LP integration (P5 gate) as a marker of Na$_V$1.5 expression.

e Percentage of mCherry positive cells after analytical flow cytometry. Homozygous and heterozygous cell lines were analyzed less than 24 hours before every SyncroPatch experiment.
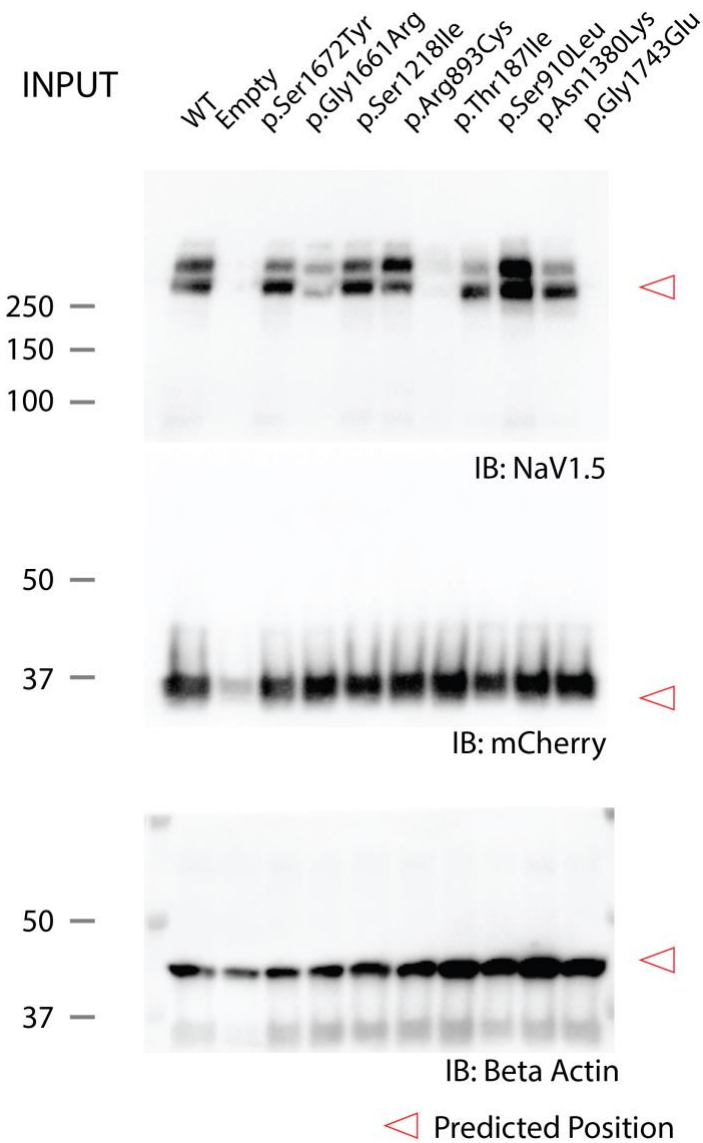
Figure S2. Western blot of selected variants. Expression of variants was assessed by Western blot for both Na$_V$1.5 and the mCherry reporter. We studied variants with no homozygous current and no dominant negative effect (p.Ser1672Tyr, p.Gly1661Arg, and p.Ser1218I), variants with no homozygous current and a weak dominant negative effect (p.Arg893Cys, p.Thr187Ile, and p.Ser910Leu) and variants with no homozygous current and a strong dominant negative effect (p.Asn1380Lys, p.Gly1743Glu). Predicted positions of bands are shown with red triangles.
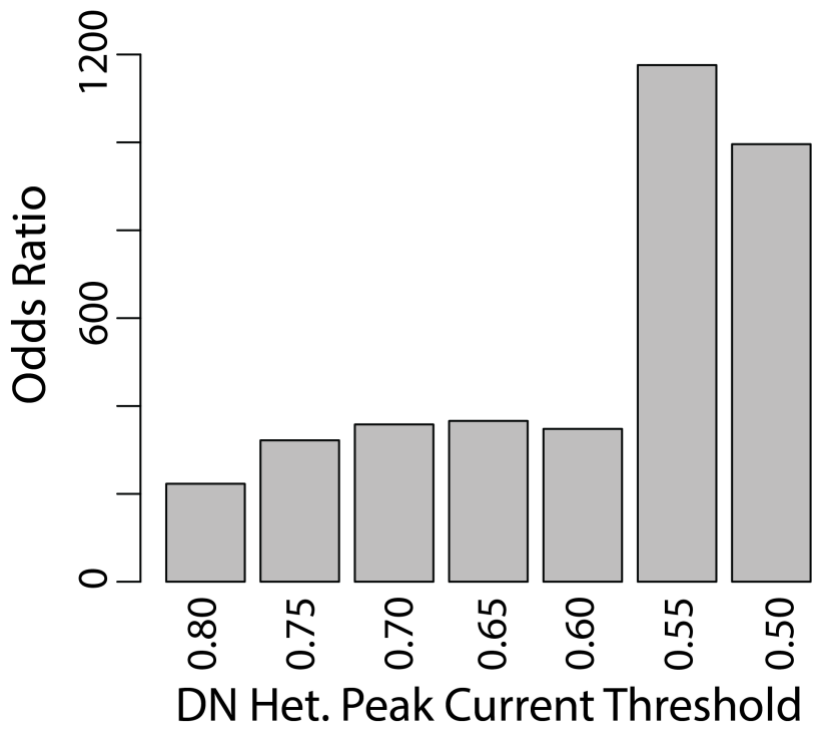
Figure S3. Sensitivity Analysis of DN Threshold. We determined the odds ratio at various heterozygous peak current thresholds among our LoF variants. We observe a consistent odds ratio between a threshold of 0.60 to 0.80, with a steep incline at cutoffs less than 0.60.
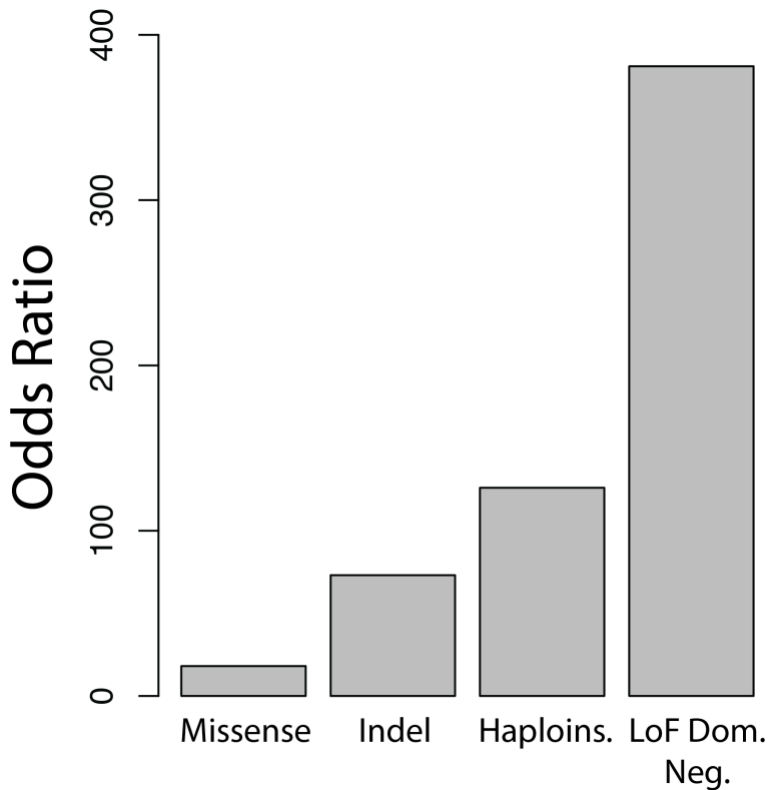
Figure S4. Odds Ratio by variant class in Non-Finnish European-ancestry individuals. Odds ratios are plotted similarly to Figure 3B restricting to NFE in gnomAD and European in the BrS consortium[7]. In this cohort, LoF DN variants have a higher enrichment compared to haploinsufficient variants (3.1 vs 2.7) but do not meet statistical significant due to lower heterozygote numbers (p = 0.0907).
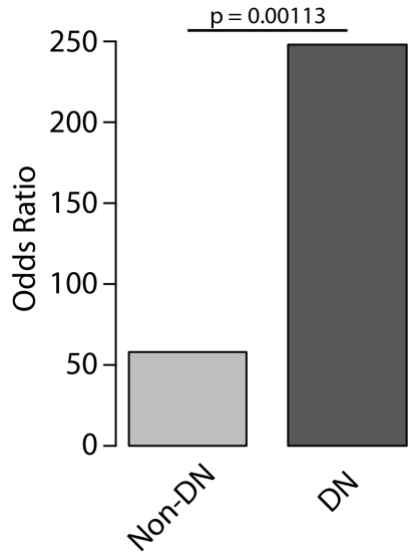
Figure S5. Odds ratios among functionally characterized dominant negative (DN) and non-dominant negative variants. Odds ratios for variants found to be non-dominant negative (N=12) vs. those found to be dominant negative (N=38) in our study.
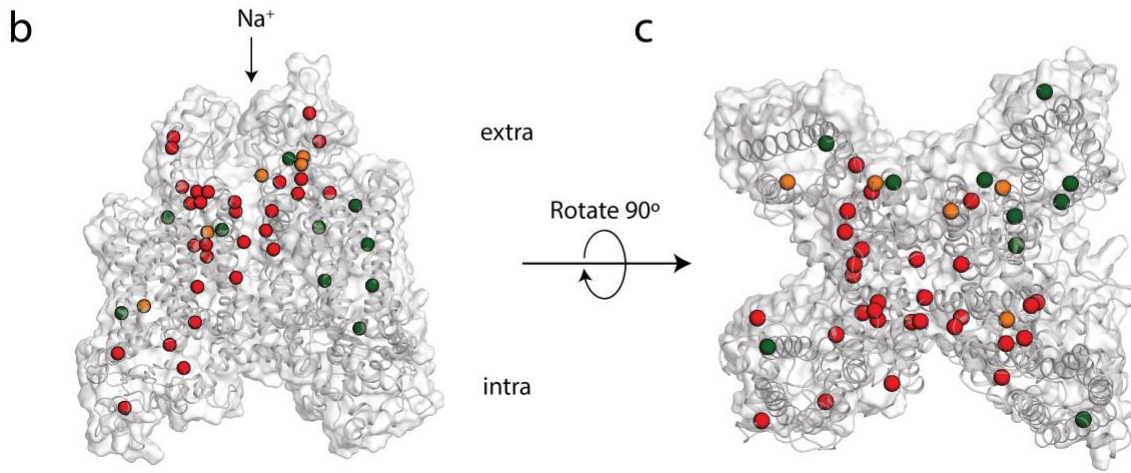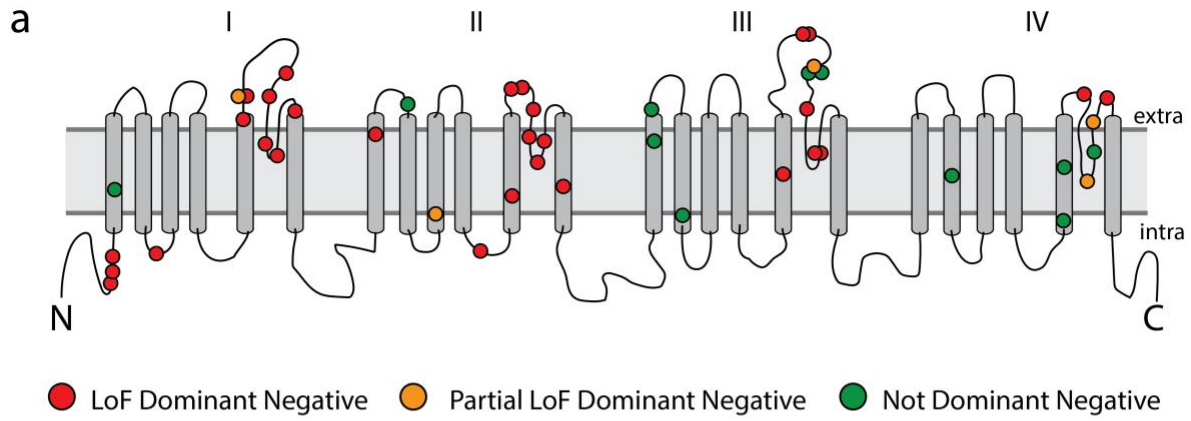
Figure S6. Structural distribution of dominant negative variants.

a Locations of dominant negative variants throughout Na$_V$1.5 in 2D channel rendering. Red indicated LoF dominant negative, orange partial LoF dominant negative, and green non-dominant negative missense variants. Extra: extracellular, intra: intracellular.

b Side view of Na$_V$1.5 protein with overlaid variant distribution.

c Top view of Na$_V$1.5 protein with overlaid variant distribution.
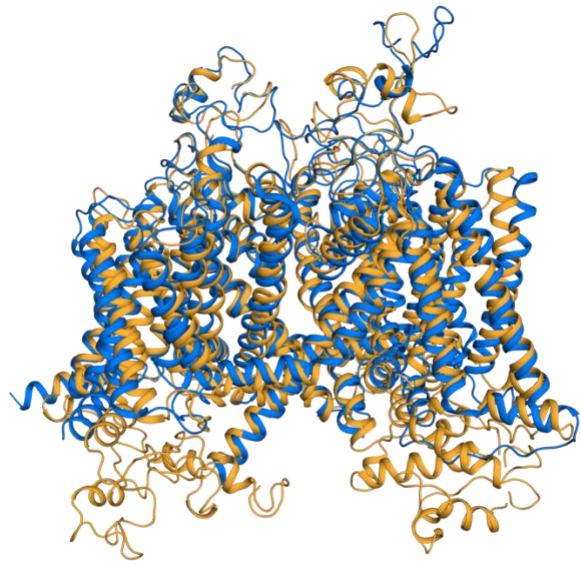
Figure S7. Structural Model and Experimental Structure. Overlay of our Nav1.5 structural model (light orange) with a recently determined cryo-EM structure of Nav1.5 (marine blue), demonstrating that our model is accurate while covering more intracellular residues than the experimental structure.

Supplemental References

1   UniProt: the universal protein knowledgebase in 2021. *Nucleic Acids Res* **49**, D480-d489, doi:10.1093/nar/gkaa1100 (2021).
2   Leaver-Fay, A. *et al.* ROSETTA3: an object-oriented software suite for the simulation and design of macromolecules. *Methods Enzymol* **487**, 545-574, doi:10.1016/b978-0-12-381270-4.00019-6 (2011).
3   Shen, H., Liu, D., Wu, K., Lei, J. & Yan, N. Structures of human Na(v)1.7 channel in complex with auxiliary subunits and animal toxins. *Science* **363**, 1303-1308, doi:10.1126/science.aaw2493 (2019).
4   Shen, H. *et al.* Structural basis for the modulation of voltage-gated sodium channels by animal toxins. *Science* **362**, doi:10.1126/science.aau2596 (2018).
5   Glazer, A. M. *et al.* High-Throughput Reclassification of SCN5A Variants. *Am J Hum Genet* **107**, 111-123, doi:10.1016/j.ajhg.2020.05.015 (2020).
6   Li, Z. *et al.* Structural Basis for Pore Blockade of the Human Cardiac Sodium Channel Na(v) 1.5 by the Antiarrhythmic Drug Quinidine*. *Angew Chem Int Ed Engl* **60**, 11474-11480, doi:10.1002/anie.202102196 (2021).
7   Walsh, R. *et al.* Enhancing rare variant interpretation in inherited arrhythmias through quantitative analysis of consortium disease cohorts and population controls. *Genet Med* **23**, 47-58, doi:10.1038/s41436-020-00946-5 (2021).